

The Influence of an Intense Laser Beam Interaction with Preformed Plasma on the Characteristics of Emitted Ion Streams

L. Láska¹, J. Badziak², S. Gammino³, K. Jungwirth¹, A. Kasperczuk², J. Krása¹, E. Krouský¹, P. Kubeš⁴, P. Parys², M. Pfeifer¹, T. Pisarczyk², K. Rohlena¹, M. Rosinski², L. Ryc², J. Skála¹, L. Torrisi³, J. Ullschmied^{1,5}, A. Velyhan¹, J. Wolowski²

¹ Institute of Physics, ASCR v.v.i., Na Slovance 2, 182 21 Prague 8, Czech Republic

² Institute of Plasma Physics and Laser Microfusion, Hery St. 23, 00-908 Warsaw, Poland

³ INFN - Laboratori Nazionali del Sud, Via S. Sofia 44, 95123 Catania, Italy

⁴ Czech Technical University, Technická 2, 16627 Prague 6, Czech Republic

⁵ Institute of Plasma Physics, ASCR v.v.i., Za Slovankou 3, 182 00 Prague 8, Czech Republic
laska@fzu.cz

Abstract

Intense laser-beam interactions with preformed plasma, preceding the laser-target interactions, significantly influence both the ion and X-ray generation. It is due to the laser pulse (its total length, the shape of the front edge, its background, the contrast, the radial homogeneity) as well as plasma (density, temperature) properties. Generation of the superfast (FF) ion groups is connected with a presence of non-linear processes. Saturated maximum of the charge states (independently on the laser intensity) is ascribed to the constant limit radius of the self-focused laser beam. Its longitudinal structure is considered as a possible explanation of the course of some experimental dependencies obtained.

1. Introduction

A laser beam, focused on solid targets, produces laser plasma that is a source of ions with various charge states and of different kinetic energy, as well as a source of X-ray radiation. The laser wavelength, the laser energy, the laser pulse length, the diameter of the focal spot and the angle of the target irradiation are factors influencing the amount and characteristics of emitted ions [1]. However, also very important is the focus setting (the position of minimum focus spot with regard to the target surface) that determines the nominal laser intensity, but also the conditions of the laser beam interaction with plasma (created by the laser pulse irradiating a target) [2].

As the plasma is produced from threshold laser intensities only of $\sim 1 \times 10^9$ W/cm² [3,4], all the laser-target interactions are preceded, primarily, by laser interactions with the pre-formed plasma of various density. Interactions of the intense laser radiation above $\sim 1 \times 10^{14}$ W/cm² with the pre-plasma (“optimum” focus position) may significantly increase the charge state and energy of the produced ions [5-8] due to the participation of various non-linear effects, including ponderomotive [9-11], relativistic [11-15] and/or magnetic [16-18] self-focusing. Such pre-plasma can be produced either by using a separate laser pre-pulse, preceding the main pulse [17,19,20], or by the main pulse itself. The self-created plasma by the front part of pulses longer than about 100 ps (with which the main part of the laser pulse interacts [5-8]), or that generated by long lasting (ns) background of very short pulses < 1 ps at a low contrast ratio [21-23], can be regarded as a pre-plasma.

Recent studies on highly charged heavy-ions generation, using the intense long pulses of the PALS high power iodine laser, operating at different experimental conditions (1ω , 3ω , various angles of the target irradiation and variable focus positions), are presented in this contribution. Because of the mentioned non-linear laser-plasma interactions, an attention is paid in a more detail also to the properties of the laser pulses themselves.

2. Experimental Arrangement

Both fundamental ($\lambda = 1.315 \mu\text{m}$) and the third ($0.438 \mu\text{m}$) harmonic frequencies of the PALS iodine laser system in Prague [24-26], with the laser pulse energies up to 560 J (1ω) and the pulse length lower than 300 ps, were used in our experiments. The Ta target was irradiated either perpendicularly, or at 30° , while the emitted ion stream was investigated at 30° (in the first case) or perpendicularly to the target (second case). The schematic view of the experimental arrangement is shown, e.g., in [27]. The minimum focus spot position with regard to the Ta target surface was varied in a broad range to make the changes of the interaction conditions of the laser beam with the self-created plasma significant. The convention used is that $\text{FP}=0$ when minimum focal spot coincides with the target surface, while $\text{FP}<0$ means that it is located in front of the target surface, and $\text{FP}>0$ means that it is inside the target. Usually, the target position was fixed, and the focusing lens was movable.

Characteristics of the ions emitted were investigated by the ion collectors (IC, ICR) and by the electrostatic ion energy analyzer (IEA) in the far expansion zone [28,29]. Soft and hard X-ray radiation from the produced plasma was monitored by the diodes with various filters [30]. A Kentech low-magnification X-ray streak camera [26] (sweep range up to 5ps/mm), placed side-on recorded radiation of energy higher than 0.8 keV, to provide time- and space-resolved information on expanding plasma radiation. Two different orientations of its entrance slits (parallel and perpendicular to the laser beam axis) provide spatial resolution of $20 \mu\text{m}$, either along the target normal or across the laser beam. Three-frame laser interferometric system with an automatic image processing [31] was used to study the plasma expansion and plasma density, both during the laser pulse and in the post interaction phase. The temporal resolution $\sim 0.3 \text{ ns}$ was determined and a spatial resolution of $\sim 20 \mu\text{m}$ was deduced [32,33].

3. Laser Pulse Properties

A good stability and a reproducibility of the PALS laser pulse-length for about 100 shots at 1ω and laser energy of 380 J, of 480 J and of $>500 \text{ J}$ is documented in **Fig.1**. Generally, the pulse length is presented as full width at half maximum (FWHM). However, considering the possible participation of the non-linear processes, further pulse characteristics are worth mentioning, because of their importance with regard to the possible laser-preformed plasma interactions. Typical shape of the leading edge of the laser pulse (in the logarithmic scale), the reproducibility of which is, however, a little bit worse, is presented in **Fig.2a**. While the contrast at -2 ns is better than 10^7 , it is about 10^6 at -1 ns and only 10^2 at -0.5 ns . Thus, at laser intensities higher than 10^{16} W/cm^2 , the expanding plasma plume appears above the target

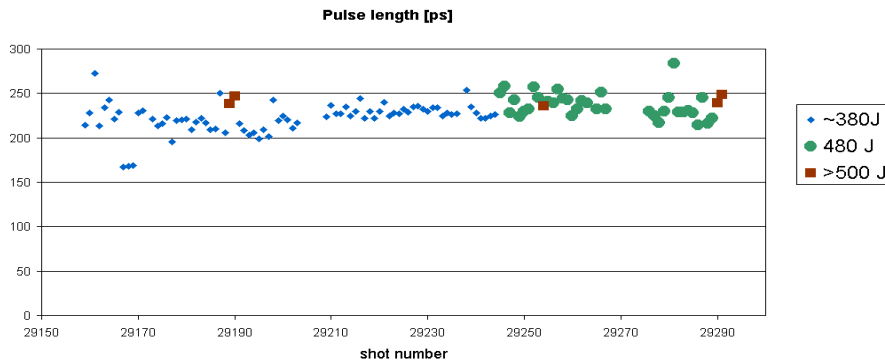


Fig. 1. Statistics of the PALS pulse-length (FWHM) for various laser energy (1ω).

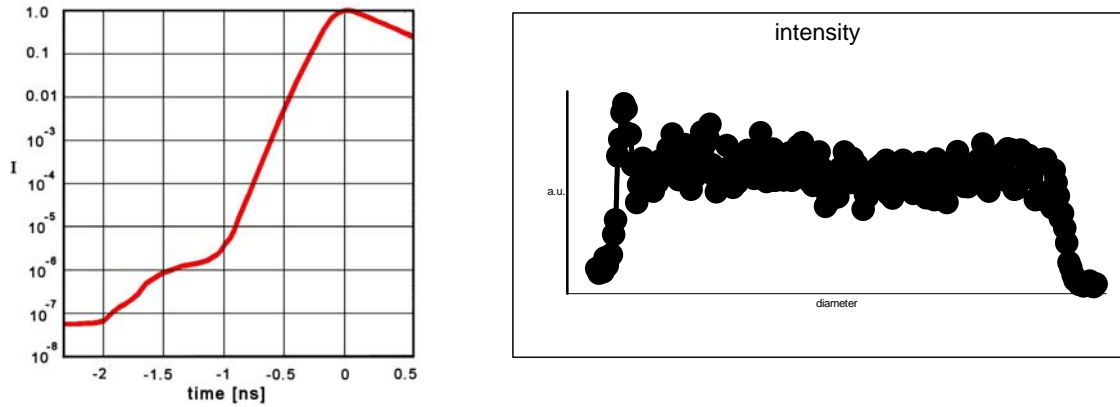


Fig.2. Front edge (a) and radial homogeneity (b) of the PALS pulse (1ω , 380 J)

surface almost ~ 2 ns before the pulse maximum, moreover, conditions for the appearance of non-linear processes may be fulfilled ~ 0.5 ns before it. Considering that the measured velocity of various emitted ion-groups range from 5×10^6 to 5×10^8 cm/s [7], the thickness of plasma layer (of varying plasma density) may attain values from tens of μm , at least, up to several of mm. For the sake of completeness, small peaks above the background plateau were recorded at 6.6 ns, 1.6 ns and 800 ps before the pulse maximum. The fall time of the pulse is about twice longer than the rising front. Such laser pulse asymmetry may influence the post-pulse plasma dynamics mainly.

The fully flat, homogeneous target irradiation by the PALS laser beam is possible in the case of the first harmonic of the laser radiation and of the laser energy below 180 J [33]. For higher energies the intensity distribution becomes concave. This is a special feature of iodine laser amplifiers that produce a stronger amplification in the off-axis region. The depth of the cavity in the center increases with increasing laser energy. For the laser energy ~ 600 J the ratio of the central intensity to that at the edge may reach the value 0.9. To obtain the same laser energy in the third harmonics, the energy of the first harmonic before the conversion should be 2-3 time higher. Thus the intensity distribution of the converted laser beam has usually a minimum in the center. After the conversion this concave character of the intensity distribution is more pronounced due to the nonlinear wavelength transformation by the DKDP crystal. In addition, the intensity distribution may not be fully symmetric across the beam diameter (**Fig. 2b**). The comparison of laser beam intensity distributions in the target plane for the first harmonic and the laser energies 100 J and 300 J, recorded by the CCD camera, was published in [32].

4. Results and Discussion

In contrast to the nominal laser pulse length (~ 300 ps), the lifetime of the expanding plasma attains values of some tens of ns. The expansion of the produced laser plasma is not isotropic with regard to the target surface – its highest velocity is in the direction of the normal to the target surface, independently of the angle of the target irradiation. Interferometric studies of plasma dynamics led even to a discovery of dense ($n_e > 10^{18} \text{ cm}^{-3}$) sharp plasma jets generated at the interaction of defocused laser beam ($I_L \sim 10^{14} \text{ W/cm}^2$) with planar metallic targets (Al, Cu, Ag, Ta, Pb) [32,33]. The jets of diameter less than 1mm are several mm long and last longer than 17 ns. A typical sequence of electron density distributions for Ta at the third harmonics

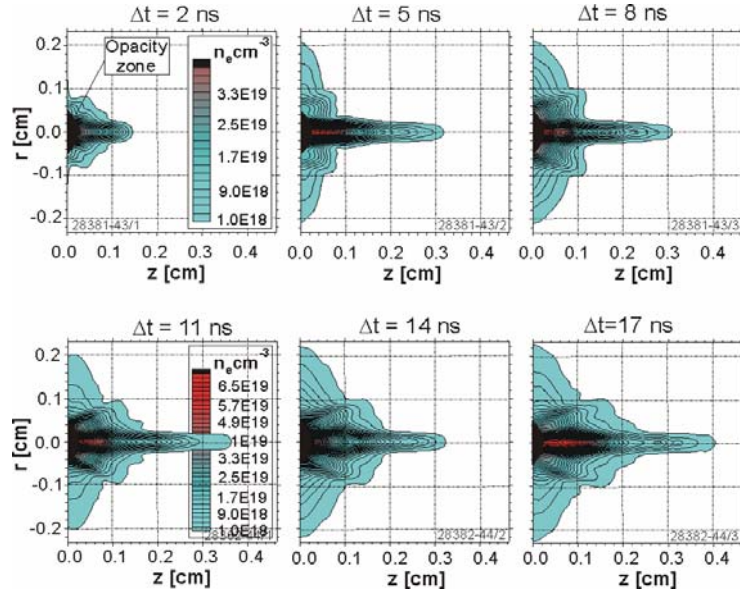


Fig.3. Expanding plasma at 2-17 ns after the target irradiation (3ω , 100 J, $FP = +300 \mu\text{m}$)

and at laser energy of 100 J is shown in **Fig. 3**, as an example. Based on dimensional analysis and 2D hydrodynamic simulation, the prevailing mechanism of jet formation was ascribed to the radiative cooling, while magnetic field should play a minor role [33].

When using the iodine laser the "optimum" focus position was found to be in front of the target surface ($FP < 0$) [34], in which ions with the highest charge states and kinetic energy can be generated (even higher than those produced in the point of the maximum nominal laser intensity). Also a significant asymmetry of various dependencies (of maximum ion charge states, ion velocities or ion kinetic energy, current of highly charged ions, crater diameters, X-ray radiation, etc.) on the FP, with regard to the position of the nominal laser intensity maximum at $FP = 0$, was recorded. This can be understood in terms of various ion accelerating processes [1,4] including non-linear processes (self-focusing) due to the laser pre-plasma interactions [2,34,35]. It is worth noticing that the new point of symmetry of the dependencies is shifted roughly to a distance of $\sim 200 \mu\text{m}$ in front of the target surface.

In **Fig. 4a** four possible combinations of laser wavelength and of angle of target irradiation, are compared. More asymmetric dependencies of z_{max} on FP were recorded for

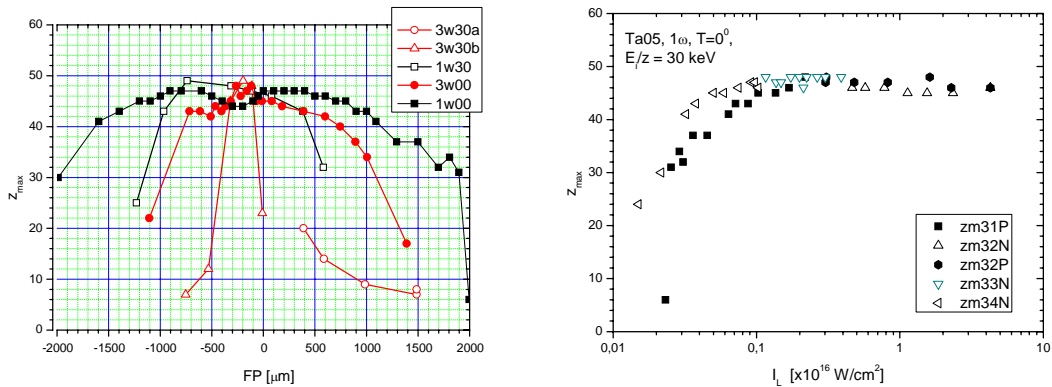


Fig.4. Maximum charge states z_{max} in dependence on the focus position.(a) and on the laser intensity (b) for combinations of 1ω , 3ω and perpendicular (00°) and 30° target angle irradiation ($P = FP > 0$, $N = FP < 0$).

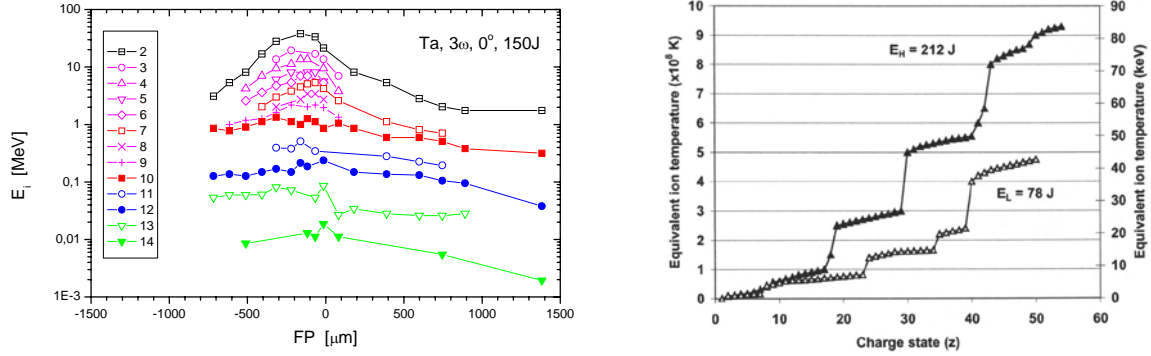


Fig.5. Peak ion energy E_i of 14 ion groups, determined from the IC signals, in dependence on the focus position FP (a) and four (five) calculated “equivalent” ion temperatures (b).

ions emitted perpendicularly to the target surface at both 1ω and 3ω (irradiation at 30°), while these dependencies for perpendicular target irradiation (ions recorded at 30°) are shifted less. This implicates an anisotropic angular emission of fast ions, which is consistent with the results in Fig.3. The fast ions with the high charge states (around 50+) and of high energy are produced also at the oblique irradiation (lower nominal laser intensity). The group of the fastest ions (with possibly higher charge states) that are emitted into a cone with the angle smaller than 30° (with regard to the target normal), cannot be recorded at the perpendicular irradiation in our experimental arrangement. We can recalculate the dependencies in Fig. 4 to those on laser intensity I_L ($I_L \lambda^2$). Generally - the higher I_L , the higher charge state and energy of produced ions. Saturation of the values of z_{\max} in a broad region of laser intensities (see Fig. 4b) implicates that the self-focusing of laser beam to the limiting diameter (of about one λ) determines the maximum attainable laser beam intensity.

Varying the laser focus position FP with regard to the target surface at a fixed laser beam energy E_L , it does not mean changes in the laser intensity only, but also changes in the interaction conditions for the laser beam that interacts with an expanding plasma plume. In Fig. 5a (3ω , 150 J) the dependencies of peak kinetic energy of fourteen ion subgroups on FP are presented that have been identified in the IC signals at various focus positions and labeled from 2 to 14. They are distributed, in principle, over three generally accepted ion groups [36,37]: slow S (13,14), thermal T (12,11) and fast F (10,7). Subgroups (9,8,6,5,4,3,2), clearly seen in the region of focus positions $-500\mu\text{m} < \text{FP} < 0$, represent a superfast (FF) ion group, which is connected with an increased intensity due to self-focusing [38]. In the region of the FP printed, the peak ion velocities range from $5 \times 10^6 \text{ cm/s}$ to $5 \times 10^8 \text{ cm/s}$, corresponding to the ion energies from $\sim 2 \text{ keV}$ to 20 MeV. The limit label 2 may represent impurities (C, O) and missing label 1 fast protons with the energy above 1 MeV. The current density of groups of the fastest ions significantly increases from the threshold value at $I_L \sim 2 \times 10^{14} \text{ W/cm}^2$ and attains maximum value up to $\sim 100 \text{ mA/cm}^2$ (1 m from the target). The duplicity of the main ion groups may be explained by astigmatism of the focusing lens, which produces, in fact, a double focus spot. A similar amount of ion subgroups was recorded at 1ω with the laser pulse energy $\sim 380 \text{ J}$.

A linear increase in the ion energy with increasing charge states characterize the ambipolar acceleration mechanism, which acts at different (low or high) plasma temperatures. The shifted Maxwell-Boltzmann-Coulomb function was used [39] to fit the measured charge-energy distribution of Ta ions (1- 54+), produced in presence of the non-linear processes. Four (five) “equivalent temperatures” with the highest one $\sim 80 \text{ keV}$ were evaluated (see Fig,

5b) that might be ascribed to four different groups of produced ions. We assume that near LTE

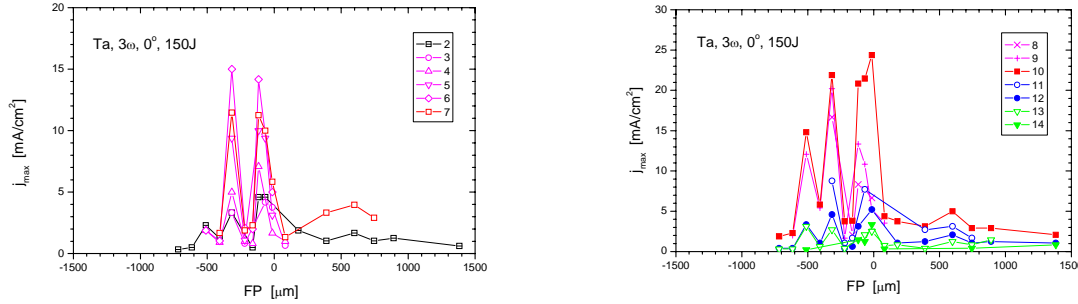


Fig.6. Relative amplitude of the current of the superfast (a) and slow, thermal and fast (b) ion groups (from the Fig.5a) in dependence on the focus position FP

conditions the developed voltage on the distance of the Debye length can be evaluated, knowing the plasma temperature and density. Calculated electric field attains a value of 6.6 MV/cm at the laser intensity of 10^{10} W/cm² and 11 GV/cm at the laser intensity of 10^{16} W/cm² [40].

By refining the course of experimental step in FP we obtained a surprising result. **Fig.6** shows a current dependence of the basic ion subgroups (8-14) on the laser focus position. Three maxima are clearly visible within the FP<0 region in front of the target. Moreover the maxima and minima of all ion subgroups coincide at the same focus positions FP, approximately, the distance of which is ~ 200 μm . This is valid also for superfast ion groups (2-7). Similar dependencies were found also for low charged ions (see Fig. 7a), the distance of peaks at FP < 0 is ~ 150 -200 μm again.

Considering that $L_{SF} \sim 200$ μm is the length necessary for the contraction of the beam, then the position of peak at FP= -500 μm indicates, in fact, the place of plasma density, sufficient for self-focusing of the laser beam at the nominal intensity $\sim 1 \times 10^{16}$ W/cm². Independent interferometric measurements [33], performed under similar experimental conditions (Ta, 3ω , 100 J) report the value of $n_e = 1 \times 10^{18}$ cm³ at the distance of 4 mm (normal to the target) even after 17 ns. It should be remembered that in FP<0 positions a front of expanding plume always meets the place of maximum laser intensity, while for FP>0 plasma expands against the laser beam with a continuously decreasing intensity than the nominal ($\sim 5 \times 10^{14}$ W/cm² at FP = +500 μm).

The amount of various kinds of ions depends on the volume of the produced plasma and its temperature. The composition of emitted plasma plume is reflected by the height of the separate ion current peaks in **Fig. 7a**. Two principal side-maxima (modulated) are dominant for ions with the charge states lower than $\sim 25+$ (similarly as for soft X-ray radiation, [41]) can be with certainty ascribed to the thermal electrons. For the higher charge states ($\sim 30+$) an independent maximum around FP = 0 appears, which is shifted for the charge states higher than 30+ to a FP<0 position. This maximum (as well as that similar for hard X-rays) is connected with the presence of fast electrons. Substantial amount of ions with the highest charge states (above 40+) were recorded only at FP<0, when conditions for the self-focusing of laser beam were met. Self-focusing lengths ~ 100 -400 μm can be estimated from the distances of the superimposed maxima; this spread might be explained by a gradually change of the laser beam intensity and of the electron density during the laser interaction within the expanding plasma plume due to the onset of self-forming.

In addition, the same maxima were found on the intensity curves of the emitted hard X-ray radiation (<20 keV) - see **Fig. 7b** (1ω , 380 J, 0^0). The emission of the both soft (0.9-7.1

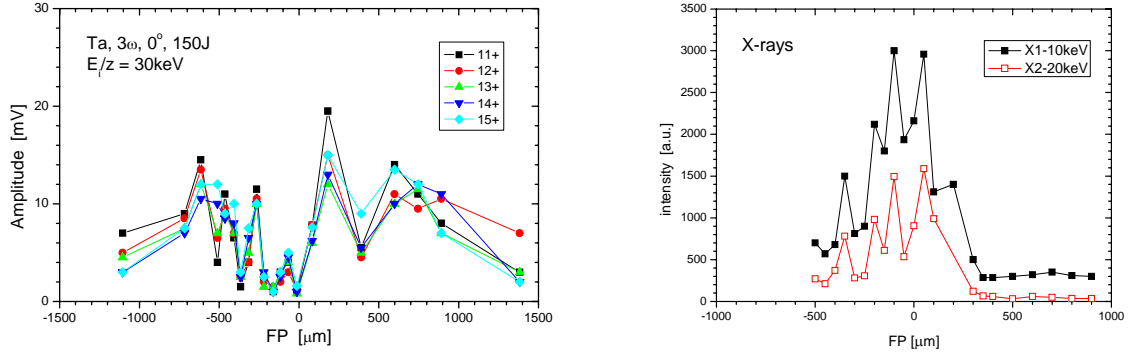


Fig.7. Relative amplitude of the low-charged single ions (a) and hard X-ray radiation (b) dependence on the focus position FP.

keV) and hard (5.1-20 keV) X-rays increases with the laser intensity. The position of the hard X-ray maximum and the maximum of the highest charged ions correlate. Both the maxima of soft X-rays are almost symmetrically positioned with regard to the hard X-ray maximum and correspond to the optimum relation of volume and temperature of produced plasma, in agreement with earlier published results [35].

The formation of a longitudinal structure of the self-focused laser beam was theoretically analyzed in [10,42]; the constriction of laser beam may not be equidistant and differs from tens to hundreds of μm . Borisov et al. [11] gave the first experimental evidence for the formation of a stable mode of spatially confined (channeled) propagation of the beam with a longitudinal structure. They observed the distribution of intensity along the filament: moon-like spots of decreasing intensity with a spatial distance $\sim 200 \mu\text{m}$.

Using the X-ray streak camera we recorded similar moon-like spots with the time distance of $\sim 100 \text{ ps}$ and with the changing intensity in the expanding plasma plume (even splitting into two plasma plumes). Examples are presented in **Fig. 8**, in which the size of the black area is about 2 ns (time-axis x) times 0.6 mm (space-axis y). The plasma produced survives several times the laser pulse length, the total length of which is, in fact, much higher than that presented as FWHM. The measured velocity of majority of emitted fast ions is $\sim 2 \times 10^8 \text{ cm/s}$ [8], it means that time distance of the bright spots $\sim 100 \text{ ps}$ could correspond to a space distance of $\sim 200 \mu\text{m}$.

Various bright spots (moon-like, half- moon-like) can be distinguished on the trace in Fig.8. The structure of the trace for the time above $\sim 800 \text{ ps}$ is not possible to ascribe to the effect of self-focused laser beam, but likely to a transformation and dissipation of the internal magnetic field. The pinching of very intense ion current beam due to very high ($\sim \text{MG}$) self-

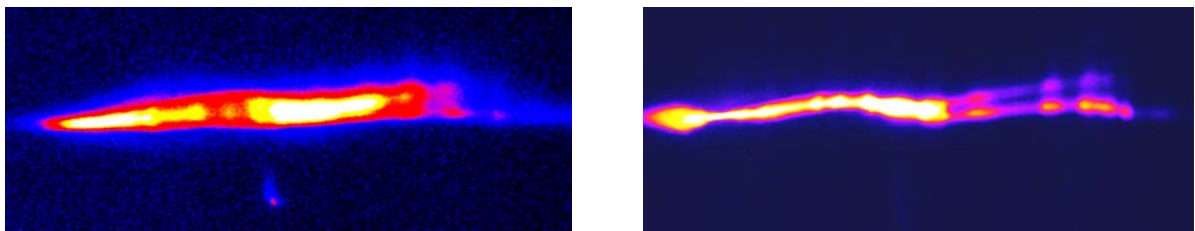


Fig.8. The X-ray streak camera image of an expanding plasma with a longitudinal structure (1ω ,

380 J, FP = +200 μm) (a) and even splitted (1 ω , 486 J, FP = -400 μm) (b).

created magnetic field [16,17] may increase the plasma temperature and consequently contribute again to the production of ions with the highest charge states and energy. Since all these phenomena proceed within ~ 2 ns, the detailed processes cannot be distinguished from each other (are integrated) in the far expansion zone (~ 2 m), of course.

5. Conclusion

It is evident that the laser target interactions are mostly accompanied (preceded) by interactions of laser beam with the pre-plasma. The pre-plasma is self-created by the main pulse – either by the front part of long pulse (>100 ps) or by the background of the short pulse (<1 ps). The lifetime of expanding plasma was proved to be about ~ 20 ns, at least. Above the intensity $\sim 1 \times 10^{14}$ W/cm² ($I\lambda^2 \sim 1 \times 10^{14}$ W/cm² μm^2) non-linear processes may start to increase the charge and the energy of the produced ions. The self-focusing increases the highest attainable laser intensities – which may be even about $\sim 10^{20}$ W/cm², however, across a very small irradiated area.

About 14 different ion groups (subgroups) were observed in the expanding plasma generated by the high power iodine laser PALS. These can be separated into four main ion groups, where the fastest one (FF) that consists of larger number of subgroups, are connected with the presence of non-linear processes. Surprisingly, oscillating dependencies of the current of single ion-groups, as well as of single (differently charged) ions and/or of X-rays on the focus position FP, were observed (maxima are separated about ~ 100 μm). These results suggest that the idea of longitudinal structure of the self-focused laser beam could be accepted, similarly, as that of pinching of very intense current beam due to a high (\sim MG) self-created magnetic field in the post irradiation phase.

The Grant Agency of the ASCR (Grant IAA 100100715) and the Ministry of Education, Youth and Sports of CR (grant LC528) kindly supported this work.

- [1] LÁSKA L. et al., XXIX. ECLIM, 2006, Madrid, Book of Abstracts, p.201, (invited); Laser Part. Beams (in press).
- [2] LÁSKA L. et al., Rev. Sci. Instrum. **75** (2004) 1588.
- [3] TORRISI L. et al., Nucl. Instr. Meth. B **184** (2001) 327.
- [4] MARGARONE D. et al., Czech. J. Phys. **56** (2006) B542.
- [5] LÁSKA L. et al., Czech. J. Phys. **54** (2004) C370.
- [6] LÁSKA L. et al., Appl. Phys. Lett. **86** (2005) 08 1502 (3).
- [7] LÁSKA L. et al., Laser Part. Beams **24** (2006) 175.
- [8] LÁSKA L. et al., Czech. J. Phys. **56** (2006) B506.
- [9] HORA H., Z. Physik **226** (1969) 159,
- [10] SUN G.-Z. et al., Phys. Fluids **30** (1978) 526.
- [11] BORISOV A.B. et al., Phys. Rev. Lett. **68** (1992) 2309.
- [12] HORA H.:J., Opt. Soc. Amer. **65** (1975) 882.
- [13] HORA H.:KANE E.L., Appl. Phys. **13** (1977) 165.
- [14] HAUSER T. et al., Phys. Rev. A **45** (1992) 1278.
- [15] HASEROTH H., HORA H., Laser Part. Beams **14** (1996) 393.
- [16] PUKHOV A., MEYER-TER-VEHN J., Phys. Rev. Lett. **76** (1996) 3975.
- [17] BORGHESI M. et al., Phys. Rev. Lett. **80** (1998) 5137.
- [18] ZVEREV E.A. et al., Plasma Phys. Rep. **31** (2005) 843.
- [19] BORGHESI M. et al., Laser Part. Beams **20** (2002) 31.

- [20] WOLOWSKI J. et al., Czech. J. Phys. **54** (2004) C385.
- [21] HATCHETT S.P. et al., Phys. Plasmas **7** (2000) 2076.
- [22] KALUZA M. et al., Phys. Rev. Lett. **93** (2004) 04500 (4).
- [23] WADA Y. et al., Jap. J. Phys. **43** (2004) L996.
- [24] JUNGWIRTH K. et al., Phys. Plasmas **8** (2001) 2495.
- [25] JUNGWIRTH K.: Laser Part. Beams **23** (2005) 177.
- [26] ULLSCHMIED J., XXIX. ECLIM, 2006, Madrid, Book of Abstracts, p. 52-60.
- [27] WOLOWSKI J. et al., Plasma Phys. Control. Fusion **45** (2003) 1087.
- [28] WORYNA E. et al., Laser Part. Beams **14** (1996) 293.
- [29] KRÁSA J., Workshop PPLA-2003, Messina, (Eds. S. Gammino, A. Mezzasalma, F. Neri, L. Torrioni), World Scientific, Hong Kong, (2004) p. 109 -117.
- [30] RYC L. et al.,: Plasma Phys. Cont. Fusion **45** (2003) 1079.
- [31] PISARCZYK et al., Czech. J. Phys. **52** (2002) D310.
- [32] NICOLAI P. et al., Phys. Plasmas **13** (2006) 062701.
- [33] KASPERCZUK A. et al., Phys. Plasmas **13** (2006) 062704.
- [34] LÁSKA L. et al., Plasma Phys. Contr. Fusion **45** (2003) 585,
- [35] LÁSKA L. et al., Rad. Eff. Def. in Solids **160** (2005) 557.
- [36] WOLOWSKI J. et al., 12 th Int. Conf. LIRPP (Osaka), 1995, AIP Conference proceedings 369, ed. S. Nakai and G. H. Miley (Woodbury, New York), p. 521.
- [37] ROHLENA K. et al., Laser Part. Beams **14** (1996) 335.
- [38] LÁSKA L. et al., Czech. J. Phys. **55** (2005) 691.
- [39] TORRISI L. et al., J. Appl. Phys. **99** (2006) 083301.
- [40] TORRISI L. et al., Czech. J. Phys. **58** (2008) B580.
- [41] TALLENTS G.J. et al., Aust. J. Phys. **39** (1986) 253.
- [42] SHARMA A. et al., J. Plasma Physics **70** (2004) 163.